Journal of Materials Chemistry A

Accepted Manuscript

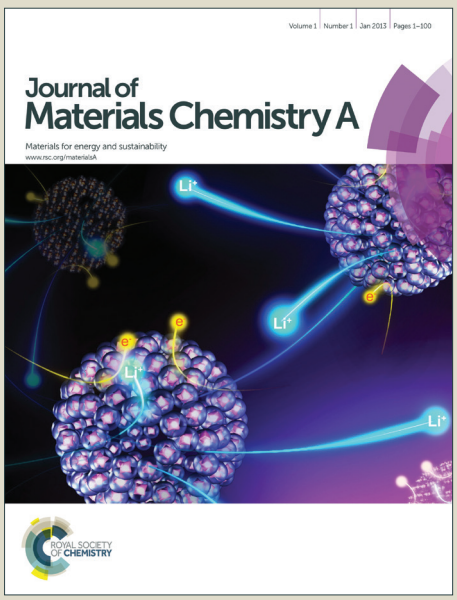

ROYAL SOCIETY OF CHEMISTRY

www.rsc.org/materialsA

Journal of Materials Chemistry A

Dynamic Article Links►

Cite this: DOI: 10.1039/c0xx00000x

ARTICLE TYPE

www.rsc.org/xxxxxx

Montmorillonite as bifunctional buffer layer material for hybrid perovskite solar cells with protection from corrosion and retarding recombination

Wenzhe Li, Haopeng Dong, Liduo Wang*, Nan Li, Xudong Guo, Jiangwei Li, Yong Qiu

Received (in XXX, XXX) XthXXXXXXXXX 20XX, Accepted Xth XXXXXXXXX 20XX
DOI: 10.1039/b000000x

4-tert-Butylpyridine (TBP) was an important component in hole transport layer for hybrid perovskite solar cells. However, our study shows that TBP can corrode the absorption perovskite layer ($CH_3NH_3PbI_3$) and interfere with the stability of the solar cells. To address this problem, montmorillonite (MMT) was used to form a buffer layer before the hole transport layer. XRD results revealed that TBP was intercalated in MMT structure and UV-vis spectroscopy analysis revealed that this structure could prevent corrosion of the $CH_3NH_3PbI_3$ layer. Moreover, the MMT buffer layer could limit the charge recombination in the solar cells. Delayed the corrosion increased the current density owing to the enhanced absorption, and a reduced charge recombination led to increased fill factor and open voltage circuit values. Consequently, the corresponding efficiency largely increased from 9.0% to 11.9% by 32.2%. Therefore, the application of MMT as a bifunctional buffer coating layer on the hole-transport layer is a useful strategy for preparing highly efficient hybrid perovskite solar cells with anti-corrosion and delayed charge recombination properties.

1 Introduction

The perovskite $CH_3NH_3PbI_3$ and its derivatives have been used as light harvesters for solar cells owing to its multiple roles of light-absorption, charge separation and transport of both holes and electrons.[1-7] Additionally, with the advantages of low costs, environmental friendliness, easy fabrication, and high efficiency, solar cells based on this type of material have potential as an ideal photoelectric device.[2, 8] Up to this point, photoelectric conversion efficiency (PCE) as high as 15% has been achieved,[9-13] which is quite close to commercial requirements.[14] The sequential deposition method raised a way to improve the loading of PbI_2 with PbI_2/N,N-dimethylformamide (DMF) solution. The more densely-packed $CH_3NH_3PbI_3$ crystals on TiO_2 films were obtained. The highest PCE of as-prepared DSSCs up to 15% with a long-term stability of maintaining 80% of the initial PCE after 500 h was obtained, which was known as the best performance.[1] The devices were commonly used the 2,29,7,79-tetrakis-(N,N-di-p-methoxyphenyl-amine)-9,99-spirobifluorene (Spiro-MeoTAD) as hole transport material (HTM) with 4-tert-butylpyridine (TBP) and bis(trifluoromethane)sulfonimide lithium salt (Li-TFSI) as additives above 12%. [15-17]

TBP is commonly used as an additive in liquid and solid state dye sensitized solar cells (DSCs), was and plays an important role on the DSC's photovoltaic performance. TBP can effectively suppress photogenerated electrons recombination from TiO_2 to electrolyte, thereby reducing energy loss.[18] Additionally, TBP can increase the polarity of the hole transporting material, improving the contacting between perovskite and hole transport layer (HTL). In the presence of TBP, the open-circuit voltage (V_{OC}) and PCEs of DSCs can be significantly improved. However, TBP is a polar solvent similar to γ-butyrolactone. Therefore TBP may be a good solvent to perovskite, which meant it can corrode the perovskite layer. To improve the overall performance of DSCs, materials capable of retarding perovskite corrosion are required.

Herein, we demonstrate that perovskite can be corroded by TBP. The corrosion process was studied by ultraviolet-visible (UV-vis) and XPS photoelectron spectroscopy. In an attempt to retard the corrosion of perovskite, montmorillonite (MMT) with an intercalated structure was introduced as a buffer layer in perovskite solar cells.[19, 20] The TBP could integrate into intercalated structure of MMT, as assessed by small-angle X-ray diffraction (SAXRD). With the modification of MMT, the stability of TiO_2/perovskite films was increased. The PCE of the fabricated devices with MMT was significant increased. The light absorption enhancement resulted in higher short circuit current (J_{SC}) values. Electrochemical impedance spectroscopy (EIS) was used to study the behavior of electrons at the interface of TiO_2/sensitizer/HTL to examine the increase of V_{OC} and fill factor (FF) in the photocurrent–voltage (J–V) curves.

2 Experiment

2.1 Solar cell fabrication and MMT treatment. The compact TiO_2 layer precursor was prepared as followings[21]: titanium (IV) isopropoxide ($Ti[OCH(CH_3)_2]_4$, 1 mL) was mixed with 2-methoxyethanol ($CH_3OCH_2CH_2OH$, 5 mL) and ethanolamine ($H_2NCH_2CH_2OH$, Aldrich, 99.8 %, 0.5 mL) and heated to 80 °C at 2 h under magnetic stirring in glove box. The TiO_2 precursor was spinning coating on the cleaned FTO at 3000 rpm for 30 s, and then the film was heated at 500 °C for 60 min to form a blocking layer. The nanocrystalline TiO_2 paste (18NRT from Dyesol Company diluted to w/w 33%) was deposited on the pre-treated FTO substrate at 7000 rpm for 30s, followed by heating at 500 °C for 1 h. The thickness of the annealed TiO_2 films were nearly 500 nm determined by scanning electron microscopy (SEM, JEOL JSM-7401F). The perovskite preparation process was followed the ref.[1] The PbI_2 (Aldrich, 99.9985%) in DMF (Aldrich, 99.9%) solution (462 mg/ml) was heated at 60 °C for 2 h under magnetic stirring stirring and the mixture was then spin coated on the as-prepared TiO_2 film at 5000 rpm for 60 s in a glove box. Then, the films were dried at 70 °C for 30 min. The dried films were dipped in a solution of CH_3NH_3I in 2-propanol (10 mg/ml) for 120 s and rinsed with 2-propanol. The films were heated at 70 °C for 30 min. After that, color of the films was dark red. The MMT dispersion was prepared by mixing 6 mg MMT solid to 1 ml chlorobenzene, filtrated with a 220 nm filter. The final concentration of the solution was one time content of 0.53 mg/mL. The 6.25% times diluted dispersion was spin coated on perovskite layer by 7000 rpm for 30s. The composition of HTM was 73 mg Spiro-MeoTAD, 17.5 uL Li-TFSI (99.95%, Aldrich)/acetonitrile solution (520 mg/mL) and 37.5 uL TBP (96%, Aldrich) in the solvent of 1 mL chlorobenzene (99.8%, Aldrich). The $CH_3NH_3PbI_3$-coated TiO_2 films were covered with HTM solution using spin-coating method at 4000 rpm for 30 s. For the counter electrode, Au (thickness: 60 nm) was deposited on the top of the HTL over layer by a thermal evaporation. The active area was fixed at 0.09 cm^2.

2.2 Characterization. UV-vis absorption spectra were employed to assess the absorption properties of perovskite sensitized TiO_2 film with a Hitachi U-3010 spectroscope. X-ray diffraction (XRD) patterns were obtained with Smart LAB instruments Cu Kα beam (λ = 1.54 Å). X-Ray photoelectron spectroscopy (XPS) was measured with a PHI 5300ESCA instrument. The Fourier transform infrared (FTIR) spectrum was measured with a Perkin-Elmer Spectrum GX FTIR spectrometer. Photocurrent–voltage *(J–V)*, Incident Photon-to-Electron Conversion Efficiency (IPCE) and Electrochemical Impedance Spectra (EIS, ranged from 0.1 Hz to 10^5 Hz) were measured by ZAHNER CIMPS electrochemical workstation, Germany.

3 Results and discussion

3.1 Perovskite corrosion mechanism by TBP

Perovskite corrosion results in a color change from black to yellow, leading to the decrease of absorption intensity. The films faded obviously upon dropping of TBP on the perovskite film in N_2 atmosphere. In our previous work, chemical corrosion of perovskite film was evidenced by decrease in light absorption, after corroded by iodine electrolytic[22] and water-oxide (UV)[23].

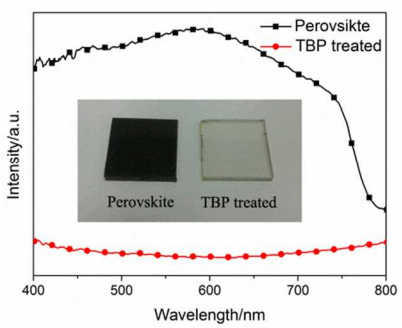

Fig. 1 UV-vis spectra of TiO_2/perovkite film and TBP treated film, the films' real photos were inserted.

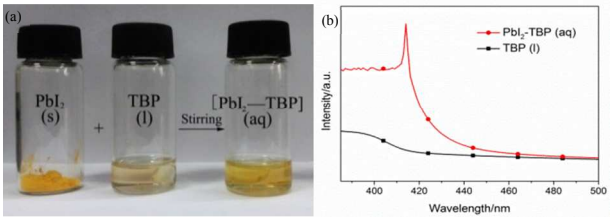

Fig. 2(a) the photograph of the reaction phenomenon between PbI_2 and TBP, (b) the UV-vis absorption of TBP liquid (dark line) and PbI_2 solution in TBP (red line)

TBP was spin coated onto the perovskite and the film's absorption was detected by UV-vis spectroscopy. The absorption results are shown in the Fig. 1. Following spin coating of TBP, the absorption decreased extremely. The results confirmed the onset of reaction between perovskite and TBP.

We then studied the reactions between PbI_2, CH_3NH_3I and TBP carefully. PbI_2 and CH_3NH_3I were mixed with TBP separately. And we found the PbI_2 reacted with TBP to form yellow liquid in room temperature, which was shown in Fig. 2a. After centrifuging at 5000 rpm for 30 min, no solid was found in centrifuge tube bottom. The yellow liquid may be attributed to PbI_2-TBP solution. TBP could dissolve 7.75% (mass percentage) PbI_2 powder in mass percentage at room temperature. The solution's light absorption curves are shown in Fig. 2b. After PbI_2 dissolved in TBP, the absorption peak located at 415 nm, relatively differed from the PbI_2 solid's[24] or TBP's absorption peak, indicating the formation of new material.

The PbI_2-TBP solution was dried under vacuum to obtain a lighter yellow powder compared with the pure PbI_2 powder. The pale-yellow powder and PbI_2 powder were investigated by XPS separately. The results were shown in Fig. 3a and b. When the TBP treated with PbI_2, the binding energy of Pb 4f7/2 shifted to lower energy level from 139.02 eV to 138.47 eV. This indicated the TBP interacted with the center lead metal, forming a complexes, like $[PbI_2 \cdot xTBP]$.

Based on the UV-vis spectra and XPS results, the degradation process can be explained as follows:

$$CH_3NH_3PbI_3\ (s) \rightleftharpoons CH_3NH_3I\ (s) + PbI_2\ (s) \quad (1\text{-}1)$$

$$PbI_2\ (s) + xTBP\ (s) \rightarrow PbI_2{-}TBP_x\ (aq) \quad (1\text{-}2)$$

$$PbI_2\ (s) + xTBP\ (s) \rightarrow [PbI_2 \cdot xTBP]\ (s) \quad (1\text{-}3)$$

In reaction 1-1, $CH_3NH_3PbI_3$ decomposes into CH_3NH_3I and PbI_2 in dynamic equilibrium. In step 1-2, the dissolution of PbI_2 in TBP leaded to PbI_2 consuming. According to Le Chatelier's principle, the degradation process preferentially proceeded in the forward direction. In steps 1-2 and 1-3 are important for the entire

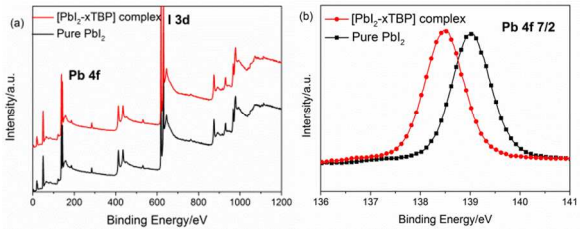

Fig. 3(a) Overall XPS spectra, (b) Pb 4f7/2 XPS spectra consuming of PbI_2.

step 1-3, TBP reacts with PbI_2 to form a pale-yellow powder that might be the $[PbI_2 \cdot xTBP]$ complex. This process also contributed to the degradation process.

To confirm that TBP could destroy the perovskite layer in the presence of the HTL, we studied the absorption of TiO_2/perovskite/HTL films with different contents of TBP in HTL. The HTL without TBP was capped on the as-prepared TiO_2/perovskite to be a blank sample. The sample containing the lowest content of TBP in HTL was denoted as "TBP*1". To strengthen the effect, a three-fold increase in the concentration of TBP in HTL was investigated, and the sample was denoted as "TBP*3". The HTL solution was spin coated on the fabricated TiO_2/perovskite films. The multi-layers of films were detected by UV-vis spectrum and the curves showed in Fig. 4. Compared with the blank sample, the TBP in HTL at the lowest content resulted in a decrease in absorption, indicating that low amounts of TBP in HTL can lead to the corrosion of $CH_3NH_3PbI_3$.

3.2 MMT as barrier for protecting corrosion by TBP

In our study, we found that MMT was a useful material to prevent perovskite corrosion by TBP in HTL. MMT was a kind of intercalation materials[25] and precious study showed that it can react with TBP to form intercalation compounds. The content of MMT buffer layer dispersion is 6.25% accorded to the v/v relative to the saturated dispersion (0.53 mg/mL). The MMT was covered on the perovskite surface through spin coating. The papered modification film and blank film (TiO_2-perovskite) were investigated by XPS to confirm the presentation of MMT. The XPS spectra were shown in Fig. S1. In modification film, the binding energy at 102.9 eV, which corresponded to Si from the tetrahedral sheets of the clay, was detected. In the O 1s region, a symmetrical band at 532.2 eV was observed which was consistent with single bonded oxygen from the silica lattice.[26] Moreover the atomic ratio of Si/Al was 4.42:1.20. This proves the MMT is presented on the perovskite surface. The thickness of MMT is indirectly characterized by a deposition of MMT on a Si slice. The atomic force microscope (AFM) figures revealed that MMT was distributed in islands with 600 nm width and 2.5 μm lengths, respectively. Through the line profile analysis, the height of the MMT sheet was ~8 nm. Kelvinprobe force microscope (KFM) was used to detect the potential difference on the sample surface. Fig. 2d and 2e respectively revealed the topo phase and potential phase of Si slices with MMT dispersed. The regions with greater height corresponded to the lower potential regions covered by the MMT sheets. Comparing Fig. S2 (f-g) with Fig. S2 (h-i), the potential differences at the perovskite surface increased obviously when MMT was added. Moreover, the dispersion and morphology of lower potential regions circled by blue lines were extremely similar to those of MMT on Si slices. Combining XPS results, we concluded that MMT partly covered the perovskite film.

Fig. 4 shows the absorption results in the presence and absence of MMT as buffer layer at varying TBP contents. At the lowest TBP content, it was easy to notice that the absorption of the sample

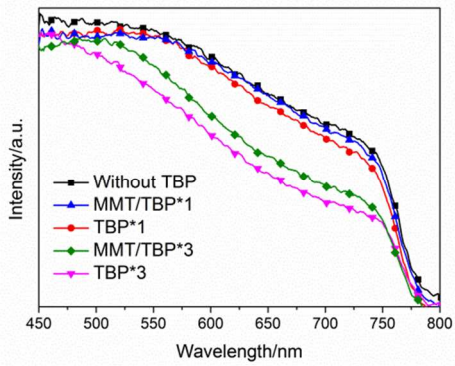

Fig. 4. UV-vis absorption of TiO_2/perovskite films without TBP treatment (black line), without (red line) and with (blue line) MMT modification capped with HTL included the TBP concentration in one times, without (green) and with (pink) MMT modification corroded by TBP in three times concentration.

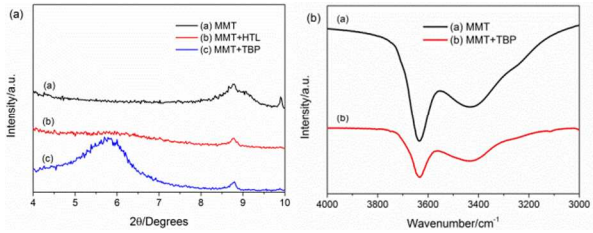

Fig. 5. (a) SAXRD spectra of MMT, MMT with HTL and MMT with TBP samples and (b) IR spectra of MMT, MMT with TBP samples

with MMT buffer layer enhanced, which was very close to that of blank sample (without TBP). When the TBP content increased by a factor of three, the absorption of films declined significantly. Moreover, the protection function of MMT was more obvious. TBP in HTL can improve the solution polarity to enhance the distribution of HTM on perovskite. Because perovskite corrosion would influence the photoelectric conversion efficiency.[22, 23] The MMT on the perovskite surface absorb TBP in its intercalated structure and inhibit direct TBP direct contacted to perovskite, which diminished corrosion efficiently.

To further study the role of MMT on inhibiting corrosion of perovskite by TBP in HTL. We firstly simulated the interaction between MMT and the HTL solution. 0.5 g of MMT was added in 0.5 ml HTL solution. The mixture was dried in the vacuum oven at 60 ^oC for 24 h. The SAXRD results in Fig 5a show an unobvious peak at ~5.70 degree. The components in the HTL solution were separately reacted with MMT to confirm the intercalation process. The results revealed that the diffraction peaks of 2θ changed from 8.78 degree to 5.70 degree after the treatment of TBP with MMT, thereby indicating that the layer spacing of MMT increased from 1.00 nm to 1.55 nm. In the HTL solution, TBP was the primary component that reacts with MMT and they formed the intercalated compound to prevent the directly contact between TBP and perovskite. The IR spectrum was performed to confirm the chemical reaction between MMT and TBP shown in Fig. 5b. Upon treatment with TBP, the absorption intensity at 3630 cm^{-1} decreased significantly. The peak location at 3630 cm^{-1} was proved to be O-H shock absorption peak in MMT.[27, 28] The intensity decrease indicated the weakening of the O-H bond in MMT. TBP contained nitrogen atoms which can form hydrogen bond with H atoms in MMT. Therefore the hydrogen bond may be the primary forces responsible for the intercalating structure in TBP.

3.3 Photovoltage performance of perovskite solar cells by adding MMT as buffer

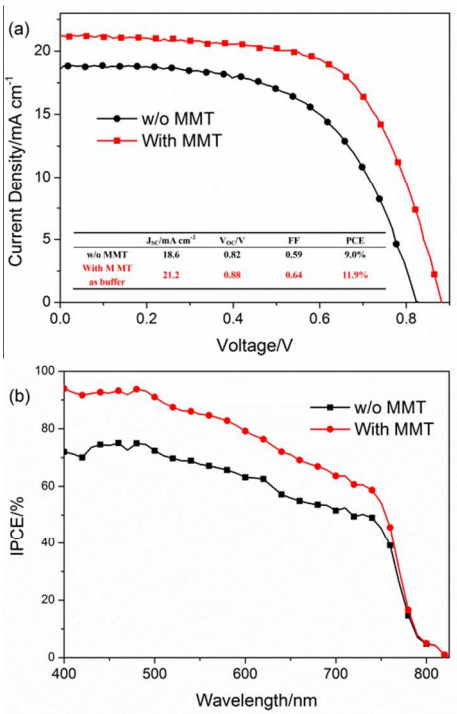

Fig. 6 (a)The J–V characteristics and (b) IPCE of devices (dark) without MMT addition and (red) with MMT addition to the HTL; the inset in (a) shown the parameter of the cells.

The solid state perovskite solar cells were fabricated using the MMT as buffer between the perovskite absorption layer and HTL in an attempt to improve device conversion efficiency. The content of MMT was optimized from 0% to 25% (v/v) accorded to the v/v relative to the saturated MMT dispersion. The PCE, V_{OC}, J_{SC} and *FF* values followed the MMT contents are shown in Fig. S3. The results show the best content is 6.25%. MMT served as a buffer coating layer on perovskite. The *J-V* curves in the presence and absence of MMT are shown in Fig. 6a. The device with MMT performed better with the PCE increasing from 9.0% to 11.9%, corresponding to a 32.2% improvement. Additionally, the J_{SC}, V_{OC} and *FF* values increased. Among the three parameters, the J_{SC} and *FF* increase significantly. Thus the MMT addition in HTL proved to be an efficient method to improve the efficiency of the perovskite sensitized all solid state solar cells. Fig. 6b shows the IPCE results. As observed, following coating with MMT, the IPCE value was obviously improved in the range of 400-750 nm from 74.5% to 92.7% as 440 nm for example.

3.3.1 Effect on J_{SC} enhancement by adding MMT as buffer

The monochromatic light conversion efficiency of the device in the range of 450–750 nm was consistent with the absorption range of perovskite. The IPCE could be expressed by the following formula (2).[29]

$$IPCE = LHE \times \phi_{inj} \times \eta_{coll} \qquad (2)$$

The three factors determining the IPCE were the light-harvesting efficiency (LHE), the quantum yield of electron injection from the excited sensitizer into the TiO_2 conduction band (ϕ_{inj}), and the collection efficiency of the photo-generated charge carriers (η_{coll}). We separately examined the three efficiency parameters of Eq. 2 to elucidate the observed higher IPCE values. The light absorption of TiO_2/perovskite film increased in the presence of MMT, as evidenced in Fig. 4, and correlates to the LHE value. MMT protected the perovskite from TBP corrosion thereby the absorption was improved. Therefore the LHE of the device was

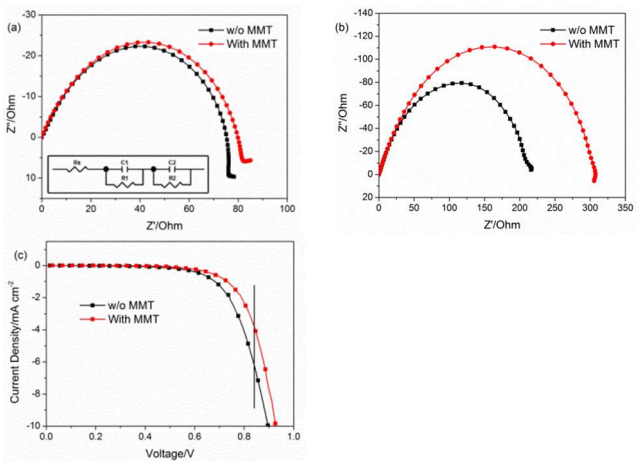

Fig.7 (a) Nyquist plots under dark condition with 0.8 V bias voltage, (b) under sun light (1.5 AM) condition and (c) the dark current curves

enhanced.

3.3.2 Effect on retarding the recombination by adding MMT in HTL

In the following studies, we noticed that MMT not only formed a blocking layer protect the perovskite from being corroded by TBP, but also retarded the charge recombination happened at the TiO_2 interface. Under full illumination, the Nyquist plot (Fig. 7a) showed typical semicircles in the frequency range of 0.1 Hz to 100 kHz. As reported in such perovskite solar cells, the resistance at the TiO_2/sensitizer/HTL interface (the R_2 in the equivalent circuit represented in Fig. 7a can be determined by the middle frequency (10–100Hz) semicircle in the Nyquist plots.[30] The values of R_2 were 49.7 Ohm and 56.9 Ohm for blank and device with MMT, respectively. The interface resistance slightly increased by 12.6%, showing that the forward electron transmission was slightly impeded. The Nyquist plot of impedance spectra in the dark under 0.8 V bias voltages revealed an increase in the resistance at the sensitized TiO_2/HTL interface (Fig. 7b). The values changed from 182.0 Ohm without MMT to 248.7 Ohm with MMT, corresponding to a 36.7% increase. The interface resistance was reflected by the obstruction of electron transmission from TiO_2 conductive band (CB) to HOMO of HTL. Generally, an increased resistance in the dark indicated restrained electron recombination. Based on the interface resistance changes under both illumination and in the dark, the recombination resistance increased much more substantially than the resistance. Furthermore, changes in *Voc* can reveal the extent of delayed electron recombination. V_{OC} can be determined using the formula below:

$$V_{OC} = \left(\frac{mRT}{F}\right) \ln\left(\frac{Isc}{I_0} - 1\right) \qquad (3)$$

where I_{SC} was the short-circuit photocurrent, i_0 is the dark current, m is the ideality factor, whose value was between 1 and 2 for perovskite solar cells, and *R* and *F* were the ideal gas and faraday constants, respectively. According to the formula, V_{OC} increases with decreasing i_0. An increased photovoltage performance and decreased dark current suggested that the dark reaction at the interface of the sensitized-TiO_2 electrode/HTL in perovskite solar cells was reduced following addition of MMT in HTL and that electron transfer from the conduction band of the TiO_2 film to the HOMO level of HTL was suppressed. Theoretically, the extent of delayed charge recombination also improves *FF* values determined from the *J–V* plot analysis, as consistent with our results.[31–33]

4 Conclusions

We demonstrated that $CH_3NH_3PbI_3$ could be corroded by TBP, which is an usual component in hole transport layer. Further studies showed that the onset of corrosion happened because TBP could dissolve PbI_2 and form [PbI_2-xTBP] complex. Consumption of PbI_2 resulted in the decomposition of perovskite. MMT was introduced to form a buffer layer on the perovskite layer. IR and XRD results showed that the MMT could interact with TBP by hydrogen bond in its intercalated structure. UV-vis results showed that the MMT could protect the perovskite from corrosion by TBP. With the addition of MMT, the corresponding efficiency of the device was improved by 32.2%, and an overall efficiency of 11.9 % was obtained under AM1.5 sunlight. The increase in J_{SC} was attributed to absorption enhancement evidenced by UV-vis measurement, owing to the delayed corrosion. The improved V_{OC} and especially *FF* values further indicated the presence of limited electron recombination processes. This was evidenced by the EIS, whereby an increase in the interface resistance in the dark was observed, and the dark current curves, whereby the dark current declined with increasing voltage. This study presents an applicable strategy for interface engineering in solid-state perovskite solar cells.

Acknowledgements

This work was supported by the National Natural Science Foundation of China under Grant no. 51273104, the National Key Basic Research and Development Program of China under Grant no. 2009CB930602.

Notes and references

Key Lab of Organic Optoelectronics & Molecular Engineering of Ministry of Education, Department of Chemistry, Tsinghua University, Beijing 100084, China

E-mail: chldwang@mail.tsinghua.edu.cn

Tel: (008610) 62788802, Fax: (008610) 62795137

1. Burschka, N. Pellet, S. J. Moon, R. Humphry-Baker, P. Gao, M. K. Nazeeruddin and M. Gratzel, *Nature*, 2013, **499**, 316-319.
2. L. Etgar, P. Gao, Z. Xue, Q. Peng, A. K. Chandiran, B. Liu, M. K. Nazeeruddin and M. Grätzel, *J. Am. Chem. Soc.*, 2012, **134**, 17396-17399.
3. H. S. Jung and J. K. Lee, *J. Phys. Chem. Lett.*, 2013, **4**, 1682-1693.
4. J. H. Heo, S. H. Im, J. H. Noh, T. N. Mandal, C. S. Lim, J. A. Chang, Y. H. Lee, H. j. Kim, A. Sarkar, K. NazeeruddinMd, M. Gratzel and S. I. Seok, *Nat. Photon.*, 2013, **7**, 486-491.
5. B. Cai, Y. Xing, Z. Yang, W.-H. Zhang and J. Qiu, *Energ. Environ. Sci.*, 2013, **6**, 1480-1485.
6. J. M. Ball, M. M. Lee, A. Hey and H. J. Snaith, *Energ. Environ. Sci.*, 2013, **6**, 1739-1743.
7. M. M. Lee, J. Teuscher, T. Miyasaka, T. N. Murakami and H. J. Snaith, *Science*, 2012, **338**, 643-647.
8. J. H. Noh, S. H. Im, J. H. Heo, T. N. Mandal and S. I. Seok, *Nano Lett.*, 2013, **13**, 1764-1769.
9. A. Kojima, K. Teshima, Y. Shirai and T. Miyasaka, *J. Am. Chem. Soc.*, 2009, **131**, 6050-6051.
10. H. S. Kim, I. Mora-Sero, V. Gonzalez-Pedro, F. Fabregat-Santiago, E. J. Juarez-Perez, N. G. Park and J. Bisquert, *Nat. Commun.*, 2013, **4**, 2242.
11. G. Xing, N. Mathews, S. Sun, S. S. Lim, Y. M. Lam, M. Grätzel, S. Mhaisalkar and T. C. Sum, *Science*, 2013, **342**, 344-347.
12. N. G. Park, *J. Phys. Chem. Lett.*, 2013, **4**, 2423-2429.
13. H. J. Snaith, *J. Phys. Chem. Lett.*, 2013, **4**, 3623-3630.
14. H. Zhang, Y. Shi, L. Wang, C. Wang, H. Zhou, W. Guo and T. Ma, *Chem. Comm.*, 2013, **49**, 9003-9005.
15. M. Liu, M. B. Johnston and H. J. Snaith, *Nature*, 2013, **501**, 395-398.
16. D. Liu and T. L. Kelly, *Nat. Photon.*, 2014, **8**, 133-138.
17. G. E. Eperon, S. D. Stranks, C. Menelaou, M. B. Johnston, L. M. Herz and H. J. Snaith, *Energ. Environ. Sci.*, 2014, **7**, 982-988.
18. L. Wang, M. Wu, Y. Gao and T. Ma, *Appl. Phys. Lett.*, 2011, **98**, 221102.
19. Y.H. Lai, C. W. Chiu, J. G. Chen, C. C. Wang, J. J. Lin, K. F. Lin and K. C. Ho, *Sol. Energ. Mat. Sol. C.*, 2009, **93**, 1860-1864.
20. Y. Geng, Y. Shi, L. Wang, B. Ma, R. Gao, Y. Zhu, H. Dong and Y. Qiu, *Phys. Chem. Chem. Phys.*, 2011, **13**, 2417-2421.
21. J. Y. Kim, S. H. Kim, H. H. Lee, K. Lee, W. Ma, X. Gong and A. J. Heeger, *Adv. Mater.*, 2006, **18**, 572-576.
22. W. Li, J. Li, L. Wang, G. Niu, R. Gao and Y. Qiu, *J. Mater. Chem. A*, 2013, **1**, 11735-11740.
23. G. D. Niu, W. Z. Li, F. Q. Meng, L. D. Wang, H. P. Dong and Y. Qiu, *J. Mater. Chem. A*, 2014, **2**, 705-710.
24. A. Ferreira da Silva, N. Veissid, C. Y. An, I. Pepe, N. Barros de Oliveira and A. V. Batista da Silva, *Appl. Phys. Lett.*, 1996, **69**, 1930-1932.
25. R. Gao, L. Wang, Y. Geng, B. Ma, Y. Zhu, H. Dong and Y. Qiu, *J. Phys. Chem. C*, 2011, **115**, 17986-17992.
26. A. P. Carvalho, C. Castanheira, B. Cardoso, J. Pires, A. R. Silva, C. Freire, B. Castro and M. B. Carvalho, *J. Mater. Chem.* 2004, **14**, 374–379.
27. B. Liu, J. Lu, Y. Xie, B. Yang, X. Wang and R. Sun, *J. Colloid Interf. Sci.*, 2014, **418**, 311-316.
28. H. Slosiariková, J. Bujdák and V. Hlavatý, *J. Incl. Phenom. Macrocycl. Chem.*, 1992, **13**, 267-272.
29. M. Grätzel, *Inorg. Chem.*, 2005, **44**, 6841-6851.
30. R. Kern, R. Sastrawan, J. Ferber, R. Stangl and J. Luther, *Electrochimi. Acta.*, 2002, **47**, 4213-4225.
31. T. Stergiopoulos, S. Karakostas and P. Falaras, *J. Photoch. Photobio. A*, 2004, **163**, 331-340.
32. A. Vittadini, A. Selloni, F. P. Rotzinger and M. Grätzel, *Phys. Rev. Lett.*, 1998, **81**, 2954-2957.
33. M. He , D. Zheng, M. Wang, C. Lin, Z. Lin. *J. Mater. Chem. A*, 2014, Advance.

TOC

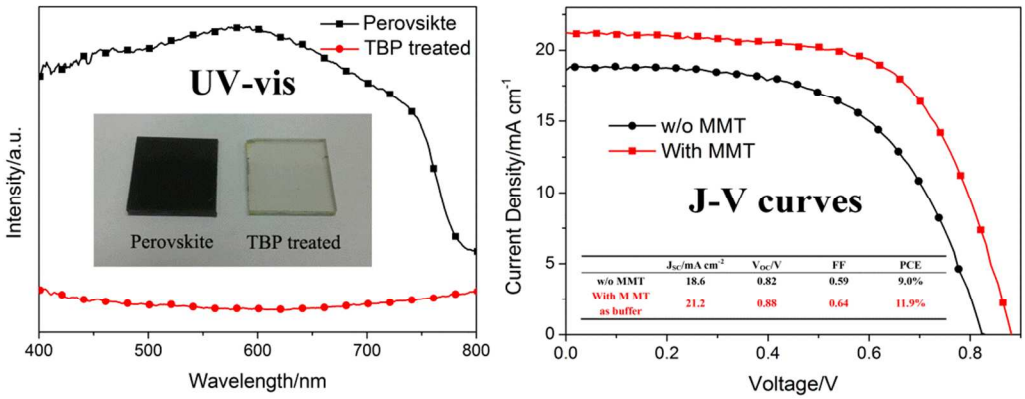

Perovskite corrosion by TBP was proved and the montmorillonite (MMT) was used as dual-functional buffer layer to prevent the corrosion and retard electron recombination.

TOC

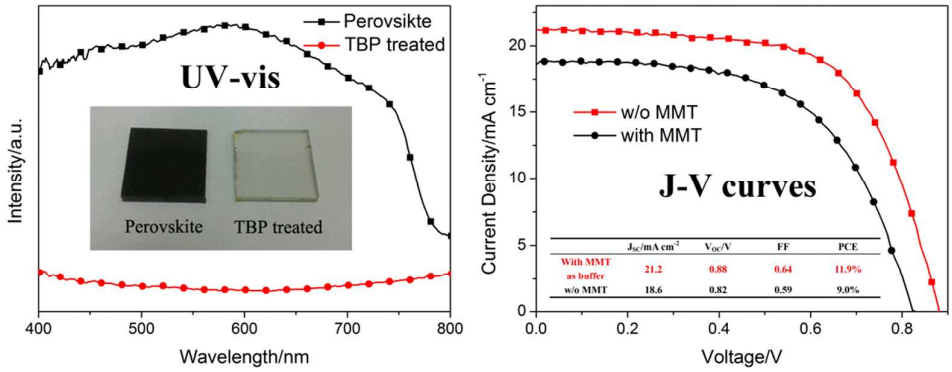

Perovskite corrosion by TBP was proved and the montmorillonite (MMT) was used as dual-functional buffer layer to prevent the corrosion and retard electron recombination.